Int. J. Econ. Environ. Geol. Vol. 13 (2) 01-08, 2022

Journal home page: www.econ-environ-geol.org

Open Access

ISSN: 2223-957X

Geology, Petrographical Features and Ore Mineralization of Volcanic Hosted Iron Ore Deposit in the Mashki Chah Area Chagai District, Balochistan, Pakistan

Shoiab Ahmed[1], Abdul Ghaffar*[1], Inayat Ullah [1], Fida Murad[1], Habib ur Rehman[2], Jalil Ahmed[3]

[1]Centre of Excellence in Mineralogy, University of Balochistan, Quetta, Pakistan

[2]National Resources Limited, Karachi, Pakistan

[3]Department of Geology, University of Balochistan, Quetta, Pakistan

*Email: ghaffar.chagai@gmail.com

Received: *20 September, 2021* ***Accepted:*** *25 May, 2022*

Abstract: The Mashki Chah iron ore deposits are located in the western Chagai magmatic belt and hosted within andesitic rock units in the Late Cretaceous Sinjrani Volcanic Group. Geometry, morphology, and structure of iron ore have massive, thin to thick-bedded and veins type of iron. The major ore type including magnetite as primary mineralization of iron ore and hematite, siderite, goethite, and limonite are secondary mineralization of iron ore. Petrographically, the iron ore is hosted within the basic to the intermediate type of units (Basaltic Andesite, Andesite, and Dacite) within the Late Cretaceous Sinjrani Volcanic Group. Major constituents of basaltic andesitic units are composed of clinopyroxene and amphibole with minor constituents of quartz. Andesitic units consist of plagioclase, hornblende, k-feldspar, quartz and biotite. The dacitic unit is comprised of quartz, albite, k-feldspar, biotite, and muscovite. SEM-EDX and BSE analysis of ore mineralization of iron ore to identify the mineral crystal structure, texture, and elemental composition of iron ore. BSE images indicate the crystal morphology of magnetite and hematite have well-developed cubic and octahedron crystal shapes with a coarse grain texture. Elemental composition is identified by the EDX graph that is indicated the high peaks of Fe and O elements associated with the high peak rock-forming minerals elements Si and O with sub-peaks of Al, Na, K, and Ca and as well as have sub-peaks of ore-forming mineral elements are include a Cu, Ag, Ti, and Sn. The total iron reserve in the deposit area is approximately about 45 to 50 million tons and an average percentage of magnetite is 86.16% and hematite is about 69.40 %. These ore deposit has significant value for economic purpose and as well as economically the Mashki Chah iron ore deposit is viable for iron ore mining.

Keywords: Mashki Chah, geology, petrography, iron ore mineralization, Chagai.

Introduction

Iron ore deposits mainly occur in numerous geological environments including sedimentary, magmatic, and hydrothermal origins (Gutzmer et al., 2009; Fard et al., 2017; Haruna et al., 2017; Nakhaei and Irannajad, 2018; Salawu and Saliu, 2021). Approximately, the world's 90% of iron ore deposits are formed in Precambrian, such as banded iron ore deposits, which are formed in sedimentary environments through chemical precipitation in early oceanic water (Klein and Beukes, 1992; Klein and Ladeira, 2000; Trendall, 2002). Another minor (10%) iron ore deposits are derived from the source of magmatism and metasomatic skarn type deposits (Broughm et al., 2017; Ovalle et al., 2018; Salazar et al., 2020; Sarjoughian et al., 2020). Various events are involved in the genesis of iron ore deposits which include diagenetic, syngenetic, and deep-seated hydrothermal processes (Sales, 1962; Ridge, 1976; Sillitoe et al., 2017).

The maturity of magmatic source of iron ore deposits has been generated from magma and lava (Farah et al. 1984; Ghasemi and Talbot, 2006). Magnetite type of iron ores are formed in dense phase magmatism which normally undergoes active gravitational settling in the magma chamber and commonly makes layers and cumulates (Edmonds et al, 2015 a; Edmonds, 2015 b; Zallmer and Edmonds, 2015 ; Ovalle et al., 2018; Edmonds and Wood, 2018). The geochemistry of magnetite can represent important information about the source deposits and the genesis of ore-forming processes (Wang et al., 2017). Magnetite is crystallized inside the andesitic magma chamber that is formed in the dominant phase of liquids. Crystallization of magnetite in these phases of liquids is conforming with the existence of multiple magnetites hosting in the clinopyroxene, the presence of basaltic andesite, and experimental phase equilibria analysis of mafic to an intermediate source of silicate magmas (Martel et al., 1999; Gaillard et al., 2003; Annen et al., 2006; Blundy et al., 2006; Rodriguez et al., 2007). The accumulation of magnetite becomes active because of different phases of magma recharge, which indicate the considerable amount of pulses of mafic magma that is injected into the hydrous andesitic magma chamber (Gualda and Anderson, 2007). The grains of magnetite in the igneous origin are ascending by the high-temperature magmatic-hydrothermal fluid that is formed the hydrothermal magnetite, which is precipitated over the primary magnetite during decompression and cooling (Simon et al., 2018).

In this study we discusses the geology, distribution, petrological characteristics, and ore mineralization of iron ore deposits with the aid of primary data of field features, petrography, and SEM-EDX characterization of iron ore mineralization.

Regional Geological Setting

The Chagai magmatic belt (CMA) is located in the western margin of Balochistan, Pakistan. It extends from the east to west direction and trends toward the eastern part of Iran about 500 km long and 150 km wide (Spector., 1981, Farah et al., 1984, Siddiqui, 2005). The CMA largely developed due to the closure of the Paleo-Tethys Ocean in the southern fragment of Laurasia (Richards, 2015). The CMA is broadly formed due to the northward subduction of the Arabian oceanic plate beneath the southern margin of the Afghan micro-continental block. Towards the north-south direction, this magmatic belt is divided into four major structural units such as; Helmand Basin, Dalbandin Basin, Mirjawa-Ras Koh Range, and Hamun-i-Mashkel depression furthermore this magmatic belt is situated about 400 km north of Makran trench and linked with Mashkel depression, Kharan forearc basin and Makran accretionary belt. (Perelló et al., 2008; Mpodozis et al., 2012; Hou and Zhang, 2015; Richard, 2015) (Fig.1). The north-east to south-west extending Balochistan volcanic arc system mainly includes three major calc-alkaline type volcanic constituents i.e., Koh-i-Sultan volcanic in the south-west of Pakistan, Koh-i-Bazman and Koh-i-Taftan south-east to the east of Iran, furthermore, these volcanic arcs have wide gap to each other (Dykstra and Birnie, 1979; Jacob and Quittmeyer, 1979; Ellouz et al., 2007; Siddiqui et al., 2010; Lemenkova, 2020).

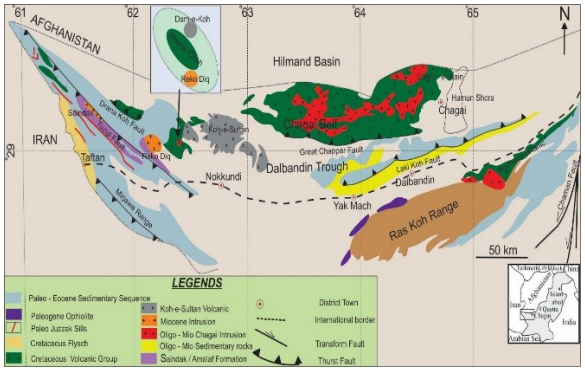

Fig. 1 Regional geological map of Chagai magmatic belt (Siddiqui, 2004; Perelló et al., 2008).

Geology of the deposits Area

Mashki Chah iron ore deposits are located about 20 Km North of Nokundi town in the western part of Chagai magmatic arc, which is covered about 80 km^2 of land area. Stratigraphically the late Cretaceous Sinjrani volcanic group is the oldest rock unit in the CMA (Arthurton et al., 1979, 1982; Siddiqui, 1996, 2004; Perelló, 2008). It is mainly dominated by submarine volcanic rocks of pyroclastic materials including breccia, volcanic conglomerate, volcanic agglomerate, tuff, and basaltic to andesitic lava flow (Ahmed et al., 1972; Siddiqui, 1996, 2004). The lower part of the Sinjrani volcanic group is not exposed and the upper part has transitional contact with Late Cretaceous to Early Plaeocene Humai Limestone (Sillitoe, 1978; Arthurton et al., 1979; Perelló et al., 2008; Nicholson et al., 2010). Late Cretaceous to Early Plaeocene Humai Limestone comprised massive thick beds of limestone with intercalated volcanic and plutonic debris associated with conglomerate (Arthurton et al., 1979, 1982; Siddiqui, 1996, 2004, 2007). Humai limestone has conformable contact with Paleocene Juzzak Formation (Hunting Survey Crop, 1960; Ahmed et al., 1972; Arthurton et al., 1979, 1982; Siddiqui, 1996, 2004). Paleo-Eocene Juzzak Formation has conformable contact with the Eocene Saindak Formation in the deposit area the Juzzak Formation is disconformable contact with the sub-recent to recent type sediments (Siddiqui, 1996, 2004).

The iron ore deposits are distributed in veins from 0.5 to 5-meter-thick on the surface within the 3km^2 area, which is composed of volcanic, plutonic, and sedimentary rock units. The volcanic rock units are broadly covered in the area of the deposit, which consists of pyroclastic materials including volcanic tuff, volcanic agglomerate, volcanic breccia, and lava flow that is comprised of basaltic, andesitic, and dacitic lava flow. The plutonic rocks are diorite, granodiorite, and granite. (Fig.2).

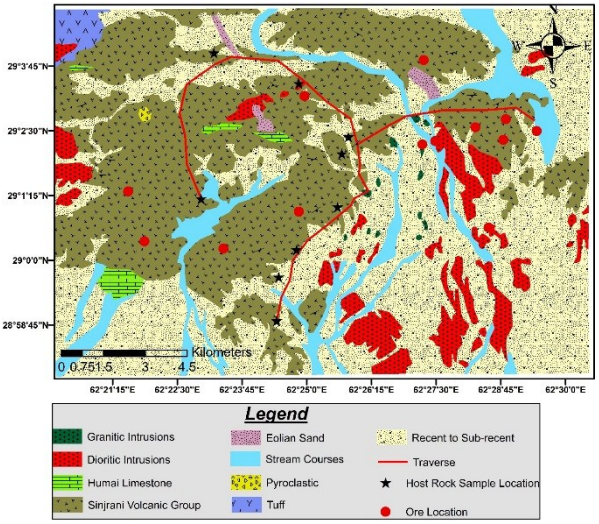

Fig. 2 Geological map of the Mashki Chah Iron Ore deposits (HSC, 1960).

Iron ore deposit in the study area is hosted within the andesitic unit of the late Cretaceous Sinjrani volcanic group and the surface color of ores is mainly black, grey, brownish red, and partly blackish brown or greyish green color. The ore of iron and hosted rock unit of iron are displaced by the fault and the trending direction of the fault from west to east direction and dip direction is about north-east (Fig.3 a). The geometry, shape, and morphology of iron ores have massive, thin to thick bed and brecciated iron ores. The massive bed of iron ore's predominant composition is hematite and magnetite. Occasionally the magnetite and hematite have mostly appeared as foliated aggregate, sometimes forming allotriomorphic aggregate, in which residual magnetite and disseminated pyrite can be observed. Magnetite is mainly hypidiomorphic and allotriomorphic distributed

mainly in a radiating lattice of hematite. The brecciated iron ores that occur in the andesitic rock units are covered by the alluvial sand (Fig.3 b and c). In the central part of the study area, the massive bed of iron is interbedded with the thin-bedded of marble with an anhydrite vein (Fig. 3 d). The types of iron ore present in Mashki Chah are mainly magnetite and hematite but in some localities in the field area, the iron ore is intensely affected by descending metroic fluids, because of the effect of metroic water the ores body is changed into the thick zone of oxidation. The oxidation zone is the main constituent of secondary ore minerals including goethite and limonite but, in some localities, the oxidation zone is associated with the supergene mineralization such as azurite and chrysocolla, thus the azurite and chrysocolla are secondary minerals, and best indicators of copper ores (Fig.3 e). The porpylitic alteration is extensively dominant in the field area, the major constituents of this alteration is consist of epidote. The color of propylitic alteration on the near-surface area appears as yellowish-green, yellowish-grey, and greyish green because weathering in some parts of the study area appears as earthy yellow. The porpylitic alteration is the best indicator of hydrothermal alteration and metasomatism in the study area it may be influences the middle to the late phase of magmatism in the Chagai magmatic belt (Fig.3 f).

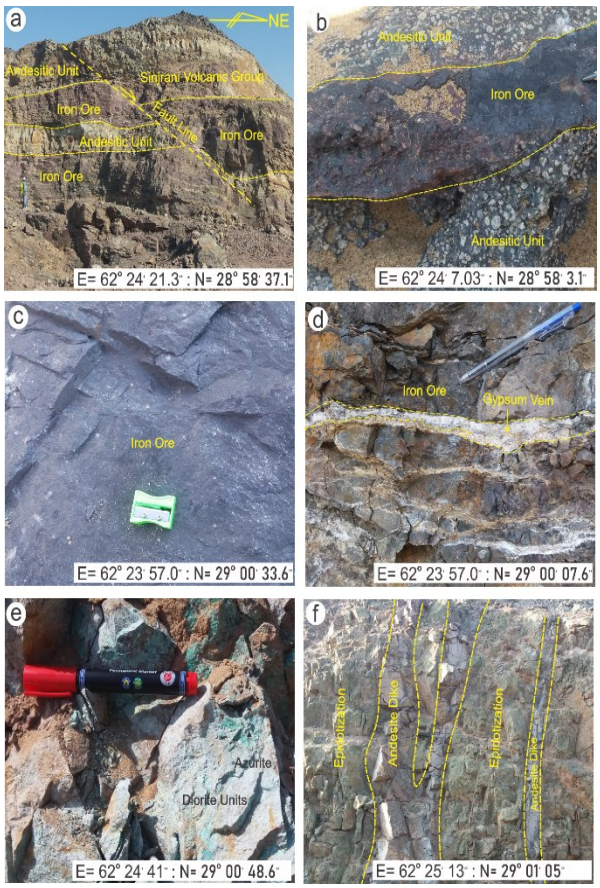

Fig. 3 (a-f): Field features of the study area. (a and b) the andesitic unit and thick bed of iron ore are displaced by the fault and brecciated iron ore is hosted within the andesitic rock units. (c and d) Thick to massive beds of iron associated with magnetite and hematite type of iron (e and f) Oxide minerals of iron (ore consist of limonite and hematite with enrichment of copper mineralization.

Materials and Methods

Throughout fieldwork demarked the ore mineralized zone, bulk sampling in the ore mineralized zone, grab samples in the host rock units, note the field feature of deposit, and as well as on the base of field data generate the geological map of the deposit area. During the geological fieldwork collected twenty-five least altered samples of host rock for the petrographic study and as well as collected ten ore-bearing or bulk type samples for the study of ore mineralization of iron. The petrographic studies were carried out by the Leica DM 500 binocular microscope attached to a digital camera. This instrument is frequently used for the identification of texture, structure, cleavage, interference figure, and other optical properties of different kinds of rock-forming minerals through reflected polarized light. Seven ore-bearing or bulk-type samples were taken for analysis of mineralization of iron ore. This investigation was accompanied by the use of Joel SEM-EDX (Model JSM 910). Such a method was utilized for the identification of ore mineral's structure, composition, and texture and also identified the other rock and ore-forming minerals chemistry associated with iron ore.

Results and Discussion

Petrography of Host rocks

Based on the visual estimation methods, all sample are plot in the field of basaltic andesite, andesite and dacite in the quartz-alkali feldspar-plagioclase (QAP) classification diagram (Fig. 4).

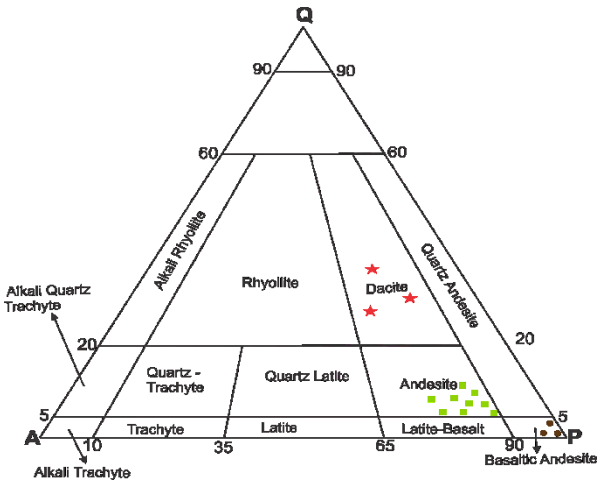

Fig. 4: QAP plot showing the relative proportions of quartz (Q), alkali feldspar (A), and plagioclase (P) in volcanic rock units in Mashki Chah Iron Ore deposit (After Gill, 2011).

Basaltic Andesite

Major constituents of basaltic andesite are mainly composed of plagioclase, pyroxene, and amphibole and a minor constituent is quartz with secondary minerals including epidote, chlorite, and sericite with iron and copper leach products and accessory minerals are apatite, zeolite and oxide minerals. Fine to coarse grain texture, coarse grain plagioclase and pyroxene,

fine to medium grains of amphiboles and fine grain quartz associated with fine to medium grains of secondary minerals with very fine grains accessory minerals are apatite and zeolite. The high interference color of pyroxene is augite bounded by the anorthite grains forming sub-intersertal texture. Phenocryst of augite has subhedral to euhedral crystal shape with inclined extinction and moderate to high fractured with high relief. Amphibole has subhedral to euhedral crystal shape with a double set of cleavages and has light greenish to brownish pleochroic and moderate relief (Fig.5 a and b).

Andesite

Major essential minerals of andesite rock units are composed of plagioclase, hornblende, clinopyroxene, alkali feldspar, quartz, and biotite. Secondary minerals in andesitic rock units are sericite, chlorite, epidote, iron leached (hematite) and copper leached associated with a secondary infilled vein of calcite. Dominant accessory minerals are appetite and oxides. Andesite has a porphyritic texture associated with phenocryst of plagioclase, alkali feldspar, and quartz and groundmasses are plagioclase, hornblende, quartz, sericite, chlorite, muscovite, and epidote associated with very fine grain accessory minerals of apatite and disseminated oxides. Plagioclase is the primary constituent of andesite and has a medium to coarse-grained texture, subhedral to euhedral crystal shape with laths crystal structure, polysynthetic albite twinning with parallel lamellae, and low to moderate relief. Quartz is the primary constituent of andesite having fine to coarse-grained texture, subhedral to euhedral prismatic crystal shape, and first-order interference color with low relief (Fig.5 c and d).

Dacite

Primary constituents of dacitic rock units mainly consist of quartz, plagioclase, biotite, alkali feldspar, and muscovite. Secondary minerals are sericite, epidote, chlorite, the vein of calcite, and copper leached (azurite), accessory minerals are apatite and zircon associated with disseminated oxides. The texture of dacite is fine with coarse grain. Quartz is a primary constituent of dacite having medium to coarse grain texture, euhedral crystal shape with prismatic crystal structure and it is highly fractured. Plagioclase is having colorless to white interference color, fine to medium grain texture, anhedral to subhedral crystal shape, and complex albite twinning. Biotite is the primary constituent of dacite which is highly pleochroic and a has a greenish to brownish interference color, fine to coarse grain texture, anhedral to euhedral crystal shape with flaky crystal structure, birds-eye extinction, and a parallel set of perfect cleavage with moderate relief. Biotite is mainly associated with muscovite (Fig.5 e and f).

Iron ore Mineralization

Magnetite (Fe_3O_4)

Magnetite is the basic element of oxides group mineral consisting of iron and oxygen. Detailed BSE, SEM-EDX analyses are identified and described the textural, composition, and structural properties of magnetite. The BSE image identified the crystal morphology, crystal structure, and texture of magnetite. Magnetite has a subhedral to euhedral crystal shape with elongated cubic crystal structure and medium to coarse grain texture (Fig.6 A-F). In this study count the 2000 to 6300 elements of Fe with 6.2 energy (KeV) and count the 7800 elements of O with 0.6 energy (KeV). This investigation specifies the high peaks of Fe and O elements, the peaks of O elements are high as compared to Fe.

Besides the high peaks of Fe and O accompanied by high peaks of rocks forming minerals elements are including a Si and O with sub-peaks of Al, Na, K, Mg ansub-peakssub ore-forminge forming minerals elements are consisting of Ag and Cu (The minimum value of Fe in the magnetite (Fe_3O_4) is about 70.42 %, the maximum value of Fe in the magnetite (Fe_3O_4) is about 98.86% and the average value of Fe in the magnetite (Fe_3O_4) is about 86.16% in the study area (Table 1).

Table 1 Showing the maximum, minimum and average value of magnetite and hematite type of iron ore from Mashki Chah iron ore deposits.

Shoot Point Data					
Mineralized Zone	**Sample No**	**O %**	**Si %**	**Al %**	**Fe %**
Magnetite	MC4-A		1.66		98.16
	MC33-A	8.93			91.07
	MC5-B	16.03	0.39	0.14	83.44
	MC4-C	15.88	2.06	0.07	79.22
	MC18- A	17.56			78.91
Average		14.6	1.37	0.105	86.16
Hematite	MC32-A	28.21			71.79
	MC7-B	29.15	0.15	0.29	70.42
	MC37-A	30.81			69.19
	MC33-A	32.05			68.54
	MC-18- B	32.13			68.47
	MC 20-A	31.98			68.02
Average		30.72167	0.15	0.29	69.405

Hematite (Fe_2O_3)

Hematite is the chief compound of oxides group mineral mainly composed of iron and oxygen. Investigation of BSE, SEM-EDX, and EDX maps determined the structural, textural, and composition properties of hematite. BSE image is recognized the crystal structure, crystal morphology, and texture of hematite. Hematite has an anhedral to subhedral crystal shape with a massive crystal structure and fine to coarse grain texture (Fig. 6 D-E). SEM-EDX analysis identified the major constituents of hematite associated with minor elements of the other minerals constituents and documented the full-fledge grains of hematite and proportion of other elements. The EDX shoot point and spectra indicate the high peaks of key elements of hematite. In this study count the 2000 to 6300 elements of Fe with 6.2 energy (KeV) and count the 7800 elements of O with 0.6 energy (KeV). This investigation specifies the high peaks of Fe and O elements, the peaks of O elements are high as compared to Fe. Besides the high peaks of Fe and O accompanied by high peaks rocks forming minerals elements are including a Si and O with sub-peaks of Al, Na, K, Mg, and Ca (Fig.6 H). The minimum percentage of Fe in hematite is about 68.02 %, the maximum percentage of Fe in hematite is 71.79% and the average percentage of Fe is about 69.40 % in the area of the deposit (Table 1).

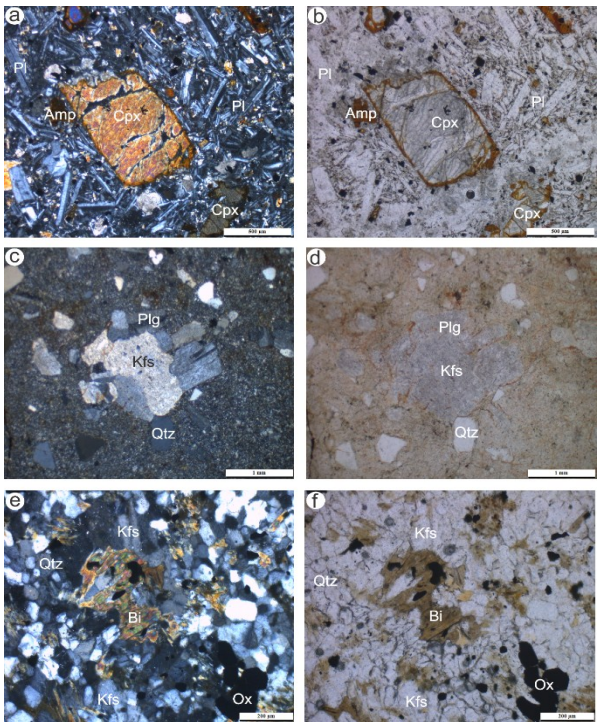

Fig. 5 (a-f) Microphotograph showing the major constituents of host rock units from Mashki Chah Iron Ore deposit. (a and b) Dark to the dark-grey color of basaltic andesite consists of porphyritic texture phenocryst is clinopyroxene and groundmasses are plagioclase and amphibole. (c and d) The light color of andesitic rock units with naked plagioclase consists of porphyritic texture, phenocryst is plagioclase and k-feldspar and groundmasses are quartz, plagioclase, and sericite with disseminated oxides. (e and f) The light color of crystalized dacite rock units consists of medium to coarse grain quartz with biotite and fine to medium-grained k-feldspar.

Iron Ore Resource

According to Nabi et al (1998), the total reserve of iron ore in Mashki Chah iron ore deposits is estimated about approximately 45 to 50 million tons deposits and the major type of iron ore minerals is magnetite and hematite. The average percentage of Fe in magnetite type of ore is about 86.16 % and hematite type ore is about 69.40 % in the study area.

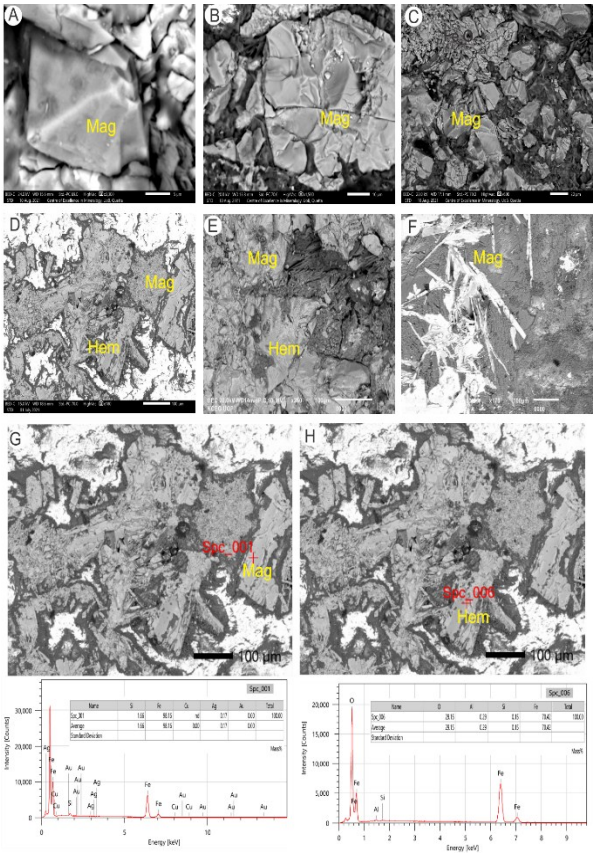

Fig. 6 (A-H). Microphotograph of Back scattered image and SEM-EDX results of magnetite and hematite type of iron ore in the study area. (A-F) Coarse grain, magnetite has euhedral well developed cubic and octahedron crystal structure associated with fine to coarse grain hematite has anhedral to subhedral crystal structure. (G and H) EDX shoot points are determined the type of iron ore (Magnetite and Hematite) with high peaks of Fe and O with sub peaks of other ore and gangue minerals elements. (Mag; Magnetite, Hem; Hematite)

Conclusion

1. Rock units are exposed in the area of the deposit mainly composed of volcanic, plutonic, and sedimentary types. The iron ore deposit in the study area is hosted within the basic to the intermediate type of rock unit within the Late Cretaceous Sinjrani Volcanic Group.

2. Host rock units in the deposit area the iron ore is hosted within the basic to intermediate rock units including basaltic andesite, andesite, and dacitic units. Major constituents of basaltic andesite are mainly composed of plagioclase, pyroxene, and amphibole and the minor constituent is quartz. Andesitic unit is containing plagioclase, hornblende, alkali feldspar, quartz, and biotite and the dacitic

unit mainly consists of quartz, plagioclase, biotite, alkali feldspar, biotite, and muscovite.

3. In the SEM-EDX analysis define the ore texture, crystal structure, and chemical composition. The major ore minerals in the study area are identified as the magnetite and hematite type of iron ore.

4. The major composition of magnetite is Fe_3O_4 and hematite is Fe_2O_3, thus the high peaks of Fe and O which indicate the major constituents of iron ore. With high peaks of Fe and O, that is indicate the Mashki Chah iron ore deposits is considered as Magnetite and Hematite types of iron ore.

5. The average percentage of iron (Fe) in magnetite type of iron ore is about 86.16 % and hematite type iron ore is about 69.40 % in the study area. Economically the iron ore deposits in Mashki Chah area are profitable as mining for industrial purpose.

References

Ahmed, W., Khan, S. N., Schmidt, R.G. (1972). Geology and copper mineralization of the Saindak Quadrangle, Chagai District, West Pakistan: U.S. *Geological Survey Professional Paper 716-A*, 21 p.

Annen, C., Blundy, J. D., Sparks, R. S. J. (2006). The genesis of intermediate and silicic magmas in deep crustal hot zones. *Journal of Petrology*, **47** (3), 505-539.

Arthurton, S. R., (1979). The geological history of the Alamreg-Mashki Chah Area, Chagai District, Balochistan. *Geodynamics of Pakistan,* 325-331.

Arthurton, R. S., Farah, A., Ahmed, W. (1982). The Late Cretaceous-Cenozoic history of western Baluchistan Pakistan the northern margin of the Makran subduction complex. *Geological Society, London, Special Publications,* **10** (1), 373-385.

Blundy, J., Cashman, K., Humphreys, M. (2006). Magma heating by decompression-driven crystallization beneath andesite volcanoes. *Nature*, **443** (7107), 76-80.

Broughm, S. G., Hanchar, J. M., Tornos, F., Westhues, A., Attersley, S. (2017). Mineral chemistry of magnetite from magnetite-apatite mineralization and their host rocks: examples from Kiruna, Sweden, and El Laco, Chile. *Mineralium Deposita*, **52** (8), 1223-1244.

Dykstra, J. D., Birnie, R.W. (1979). Segmentation of the Quaternary subduction zone under the Baluchistan region of Pakistan and Iran, in Farah, A., and De Jong, K.A., eds., Geodynamics of Pakistan: Quetta, Geological Survey of Pakistan, p. 319–323.

Edmonds, M. (2015 a). Research Focus: Flotation of magmatic minerals. *Geology*, **43** (7), 655-656.

Edmonds, M., Brett, A., Herd, R. A., Humphreys, M. C. S., Woods, A. (2015 b). Magnetite-bubble aggregates at mixing interfaces in andesite magma bodies. *Geological Society, London, Special Publications*, **410** (1), 95-121.

Edmonds, M., Woods, A. W. (2018). Exsolved volatiles in magma reservoirs. *Journal of Volcanology and Geothermal Research*, **368**, 13-30.

Ellouz-Zimmermann, N., Deville, E., Müller, C., Lallemant, S., Subhani, A. B., Tabreez, A. R. (2007). Impact of sedimentation on convergent margin tectonics: Example of the Makran accretionary prism (Pakistan). In *Thrust belts and foreland basins* (pp. 327-350). Springer, Berlin, Heidelberg.

Farah, A., Lawrence, R. D., DeJong, K. A. (1984). An overview of the tectonics of Pakistan. *Marine geology and oceanography of Arabian Sea and Coastal Pakistan. Van Nostrand Reinhold Company, New York*, 161-176.

Gaillard, F., Schmidt, B., Mackwell, S., McCammon, C. (2003). Rate of hydrogen–iron redox exchange in silicate melts and glasses. *Geochimica et Cosmochimica Acta*, **67** (13), 2427-2441.

Ghasemi, A., Talbot, C. J. (2006). A new tectonic scenario for the Sanandaj–Sirjan Zone (Iran). *Journal of Asian Earth Sciences*, **26** (6), 683-693.

Gualda, G. A., Anderson, A. T. (2007). Magnetite scavenging and the buoyancy of bubbles in magmas. Part 1: Discovery of a pre-eruptive bubble in Bishop Rhyolite. *Contributions to Mineralogy and Petrology*, **153** (6), 733-742.

Gutzmer, J., Beukes, N. J., De Vivo, B., Grasemann, B., Stüwe, K. (2009). Iron and manganese ore deposits: mineralogy, geochemistry, and economic geology. *Encyclopedia of Life Support Systems. UNESCO, Paris*, 43-69.

Haruna, A. I., Umar, U. S., Mohammed, A. A., Maude, K. A (2017). Geochemistry and Economic Potential of Jaruwa Iron Ores, NW-Nigeria. *Imperial Journal of Interdisciplinary Research,* volume (3), 1067-1074.

Hou, Z., Zhang, H. (2015). Geodynamics and metallogeny of the eastern Tethyan metallogenic domain. *Ore Geology Reviews*, *70*, 346-384.

Hunting Survey Corporation, (1960). Reconnaissance Geology of part of West Pakistan. A Colombo Plan Cooperation Project, Toronto, Canada, 550.

Jacob, K.H., Quittmeyer, R. L. (1979). The Makran region of Pakistan and Iran: Trench-arc system with active plate subduction, in Farah, A. and De Jong, K.A., eds., Geodynamics of Pakistan: Quetta, *Geological Survey of Pakistan*, 305–317.

Klein, C., Beukes, N. J. (1992). Proterozoic iron-formations. In: *Developments in Precambrian Geology,* Elsevier, **10**, 383-418.

Klein, C., Ladeira, E. A. (2000). Geochemistry and petrology of some Proterozoic banded iron-formations of the Quadrilátero Ferrífero, Minas Gerais, Brazil. *Economic Geology*, **95** (2), 405-427.

Lemenkova, P. (2020). The geomorphology of the Makran Trench in the context of the geological and geophysical settings of the Arabian Sea. *Geology, Geophysics and Environment*, **46** (3), 205-222.

Martel, C., Pichavant, M., Holtz, F., Scaillet, B., Bourdier, J. L., Traineau, H. (1999). Effects of f O2 and H2O on andesite phase relations between 2 and 4 kbar. *Journal of Geophysical Research: Solid Earth*, **104** (B12), 29453-29470.

Mpodozis, C., Cornejo, P. (2012). Cenozoic tectonics and porphyry copper systems of the Chilean Andes. *Society of Economic Geologists Special Publication*, **16**, 329-360.

Nakhaei, F., Irannajad, M. (2018). Reagents types in flotation of iron oxide minerals: A review. *Mineral Processing and Extractive Metallurgy Review*, **39** (2), 89-124.

Nicholson, K. N., Khan, M., Mahmood, K. (2010). Geochemistry of the Chagai–Raskoh arc, Pakistan: Complex arc dynamics spanning the Cretaceous to the Quaternary. *Lithos*, **118** (3-4), 338-348.

Ovalle, J. T., La Cruz, N. L., Reich, M., Barra, F., Simon, A. C., Konecke, B. A. Morata, D. (2018). Formation of massive iron deposits linked to explosive volcanic eruptions. *Scientific reports*, **8** (1), 1-11.

Perelló, J., Razique, A., Schloder, J., (2008). The Chagai porphyry copper belt, Baluchistan province, Pakistan. *Economic Geology,* **103** (8*), 15 83-1612.*

Richards, J. P. (2015). Tectonic, magmatic, and metallogenic evolution of the Tethyan orogen: From subduction to collision. *Ore Geology Reviews*, **70**, 323-345.

Ridge, J. D. (1976). Origin, development, and changes in concepts of syngenetic ore deposits as seen by North American Geologists1. In *Classifications and Historical Studies* (pp. 183-297). Elsevier.

RodrÍguez, C., Sellés, D., Dungan, M., Langmuir, C., Leeman, W. (2007). Adakitic dacites formed by intra crustal crystal fractionation of water-rich parent magmas at Nevado de Longaví volcano (36· 2 S; Andean Southern Volcanic Zone, Central Chile). *Journal of Petrology*, **48** (11), 2033-2061.

Salawu, S. I., & Saliu, A. M. (2021). Characterization and beneficiation of Obajana iron ore, Kogi State, Nigeria. *Acta Technica Corviniensis-Bulletin of Engineering*, **14** (4), 105-108.

Salazar, E., Barra, F., Reich, M., Simon, A., Leisen, M., Palma, G. Rojo, M. (2020). Trace element geochemistry of magnetite from the Cerro Negro Norte iron oxide− apatite deposit, northern Chile. *Mineralium Deposita*, **55** (3), 409-428.

Sales, R. H. (1962). Hydrothermal versus syngenetic theories of ore deposition. *Economic Geology*, **57** (5), 721-734.

Sarjoughian, F., Habibi, I., Lentz, D. R., Azizi, H., & Esna-Ashari, A. (2020). Magnetite compositions from the Baba Ali iron deposit in the Sanandaj-Sirjan zone, western Iran: Implications for ore genesis. *Ore Geology Reviews*, *126*, 103728.

Siddiqui R H., (1996). Magmatic evolution of Chagai-Raskoh arc terrane and its implication for porphyry copper mineralization. *Geologica,* **2**, 87-119.

Siddiqui R H. (2004). Crustal evolution of the Chagai-Raskoh arc terrane, Balochistan, Pakistan. Ph.D. Thesis, Centre of Excellence in Geology, University of Peshawar, Pakistan.

Siddiqui R H., Asif Khan, M., Qasim Jan, M. (2005). Petrogenesis of Eocene Lava flows from the Chagai Arc, Balochistan, Pakistan, and its tectonic implications. *Journal of Himalayan Earth Sciences,* **38,**163-187.

Siddiqui, R. H., Asif Khan, M., Qasim Jan, M. (2007). Geochemistry and petrogenesis of the Miocene alkaline and sub-alkaline volcanic rocks from the Chagai arc, Baluchistan, Pakistan: Implications for porphyry Cu-Mo-Au deposits. *Journal of Himalayan Earth Sciences*, **40**, 1-23.

Siddiqui, R. H., Khan, M. A., Jan, M. Q., Brohi, I. A. (2010). Paleocene tholeiitic volcanism and oceanic island arc affinities of the Chagai Arc, Balochistan, Pakistan. *Sindh University Research Journal-SURJ (Science Series)*, **42** (1), 83-98.

Sillitoe, R. H. (1978). Metallogenic **42**evolution of a collisional mountain belt in Pakistan: a preliminary analysis. Journal of the Geological Society, **135** (4), 377-387.

Sillitoe, R. H., Perelló, J., Creaser, R. A., Wilton, J., Wilson, A. J., Dawborn, T. (2017). Age of the Zambian Copper belt. *Mineralium Deposita*, **52** (8), 1245-1268.

Simon, A. C., Knipping, J., Reich, M., Barra, F., Deditius, A. P., Bilenker, L., Childress, T. (2018). Kiruna-type iron oxide-apatite (IOA) and iron oxide copper-gold (IOCG) deposits form by a combination of igneous and magmatic-hydrothermal processes: evidence from the Chilean Iron Belt.

Spector, A., (1981). Report on interpretation of aeromagnetic survey data of Baluchistan Province, Pakistan. *Allan Spector and Associates Ltd., Canada*.

Trendall, A. F. (2002). The significance of iron-formation in the Precambrian stratigraphic record. *Precambrian sedimentary environments: A modern approach to ancient depositional systems*, 33-66.

Wang, F., Bagas, L., Jiang, S., Liu, Y. (2017). Geological, geochemical, and geochronological characteristics of Weilasituo Sn-polymetal deposit, Inner Mongolia, China. *Ore Geology Reviews*, **80**, 1206-1229.

Zellmer, G. F., Edmonds, M., Straub, S. M. (2015). Volatiles in subduction zone magmatism. *Geological Society, London, Special Publications*, **410** (1), 1-17.